Adsorption kinetics, equilibrium and thermodynamics of gas-phase toluene onto char produced from almond shells

Sinan Kutluay, Orhan Baytar, Ömer Şahin

Research Article

Adsorption kinetics, equilibrium and thermodynamics of gas-phase toluene onto char produced from almond shells

Sinan Kutluay[*,a], Orhan Baytar[b], Ömer Şahin[c]

Department of Chemical Engineering, Siirt University, Siirt, Turkey

Article Info	Abstract
	Toluene is the primary material in chemical process industries and is often used as a raw material in the production of many chemicals and as a solvent in many engineering processes. In this study, the material of char, which is used as an adsorbent, was produced from almond shells. The adsorption process of gas-phase toluene onto char was investigated using a laboratory-scale fixed-bed reactor under atmospheric pressure. The structure of the char was characterized by BET and FTIR. The influences of adsorption parameters such as nitrogen (N_2) flow rate as the gas-phase toluene carrier, char amount, gas-phase toluene concentration at the inlet and the adsorption temperature on both the adsorption capacity and adsorption efficiency were examined. It was found that the adsorption of the gas-phase toluene onto char could be well represented by the pseudo-second-order kinetic model. Equilibrium isotherm data were analyzed by the Langmuir and Freundlich isotherm models and the results indicated that the adsorption process was described well by the Langmuir isotherm model. The maximum monolayer adsorption capacity (q_{max}) of the char was determined as 15.42 mg g^{-1} for 303 K. Thermodynamic parameters such as $\Delta G° = -7.93$ kJ mol^{-1}, $\Delta H° = -17.18$ kJ mol^{-1}, $\Delta S° = -0.013$ kJ mol^{-1} K^{-1} showed that the adsorption process was spontaneous, exothermic and physical. The results showed that the material of char produced from almond shells could be used as a biosorbent to remove the material of gas-phase toluene from various industrial and natural sources through the adsorption method.

1. Introduction

Volatile organic compounds (VOCs) are important air pollutant components which are found in the atmosphere and originate from all municipal and industrial areas [1]. VOCs are pollutants that are emitted to the environment from chemicals, petrochemicals and many other industries. There are numerous sources of VOCs including the evaporation of chemicals such as solvents, thinners, scrubbers and lubricants, flue gas emissions from the burning of fossil fuels for industrial and urban activities and the incineration of wastes resulting from urban life, oil refineries and stations, etc. [2-5]. VOCs are not removed before being released to the environment and have serious detrimental effects on the environment and thus on living things [6]. VOCs, which can readily mix into the air with direct evaporation, can lead to fatalities when inhaled. Various VOCs can cause persistent health problems due to their negative properties. VOCs accumulate on the leaves and refined crops which, in turn, affects photosynthesis. Other VOCs, which are carcinogenic, can lead to death by intoxication [3]. The most common VOCs are benzene, toluene, ethylbenzene and xylene, collectively known as BTEX. These VOCs are particularly notable due to their health risks. Toluene is within the group of components that do not carry

cancer risk. The most important health risk of toluene is its acute and chronic effects on the central nervous system. Toluene is a VOC that is abundantly found in the environment as it is the primary material in chemical process industries and often used as a raw material in the production of many chemicals and as a solvent in many engineering processes [7]. Toluene has been reported to cause indoor and outdoor pollution even at low concentrations in its gas-phase [8].

There are many processes used in the removal of VOCs such as thermal and catalytic combustion, biofiltration absorption, condensation, thermal oxidation, catalytic oxidation and adsorption. Among VOC removal and recovery techniques, the nondestructive adsorption process which has many advantages in terms of process conditions and applicability is one of the most appropriate and preferred methods for removing VOCs [3, 9, 10]. The adsorption process is a useful technology for the separatin and removal of VOCs because it can be developed with relatively low cost in addition to providing flexibility and simplicity in process design, operations and maintenance [11, 12]. Furthermore, the adsorption process is a renewable process that is the least harmful [13, 14]. This technique of adsorbing the VOCs provides high efficiency in the removal of solvents and VOCs both at low and high concentrations [14]. Adsorption is usually carried out on a fixed-bed filled with adsorbents. There are many studies on fixed bed modeling in the literature [15, 16]. Allen et al. [17] developed theoretical mathematical equations for the adsorbed in the adsorbent particles given by injection to a gas stream. The equations in their study were solved using parameters such as different gas flow rate and adsorbent feed rate and the results were analyzed. In other studies, theoretical and experimental results were evaluated together [18, 19]. Various solid materials used as adsorbents in the adsorption process have a porous structure and the inner surface areas are larger than the outer surface areas. The adsorption on the inner surface of the layer does not occur as easily as it does on the outer surface. This is because gas molecules interact with atoms, molecules or ions when entering the surfaces. When this occurs, condensation takes place in the inner surface which is called capillary condensation. Adsorption can take place in the form of physical adsorption, otherwise known as van der Waals adsorption, or chemical adsorption, otherwise known as chemisorption [13, 14, 20].

Almond shells, which are abundant and low-cost residues, are suitable for being used as raw materials for the preparation of char. Material for char is produced by heating biomass in the total or partial absence of oxygen. Pyrolysis is the most common technology employed to produce char and also occurs in the early stages of the combustion and gasification processes.

In the literature, there are no studies conducted on the adsorption of gas-phase toluene onto char produced from almond shells in a dynamic system. For this reason, within the context of the main purpose of this study, the effects of adsorption parameters such as the flow rate of nitrogen (N_2) as the gas-phase toluene carrier, char amount, gas-phase toluene concentration at the inlet and the adsorption temperature, which are important in the adsorption process, were examined and the results were optimized using gas chromatography method. In addition, adsorption kinetics, isotherms and thermodynamics of the gas-phase toluene onto char were investigated at different temperatures.

2. Materials and Method

2.1. Materials

The almond shells used in this study were obtained from the province of Siirt which is located in the South-East of Turkey. The almond shells were ground in a mortar and sieved to a particle size of -500+125 μm. The obtained samples were stored in closed containers

to be used in char production. The adsorbate used in this study was analytical grade toluene (Sigma Aldrich, 99.0%).

2.2. Production of Char

The production of char from almond shells was carried out in a vertical electric furnace. In the production process of the char, the almond shells (100 g) with a particle size of -500+125 μm were placed in a ceramic crucible bowl and pyrolyzed at 350°C for 30 min in a box furnace. The heating rate was not controlled but was consistently 8-10°C/min through the heat-uptime. N_2 of 99.9% purity was used as a sweep gas in the furnace to prevent oxygen from entering. After pyrolysis, the material was allowed to cool overnight in the furnace with nitrogen as the sweep gas. The obtained material was kept in closed bottles to be used in the experimental studies.

2.3. Dynamic Adsorption Process of Gas-Phase Toluene onto Char

The experimental setup used in the adsorption studies is schematically shown in Figure 1. The gas-phase toluene adsorption experiments of the char adsorbent were performed in the fixed bed of a Pyrex-glass reactor with a height of 16 cm and an internal diameter of 0.9 cm.
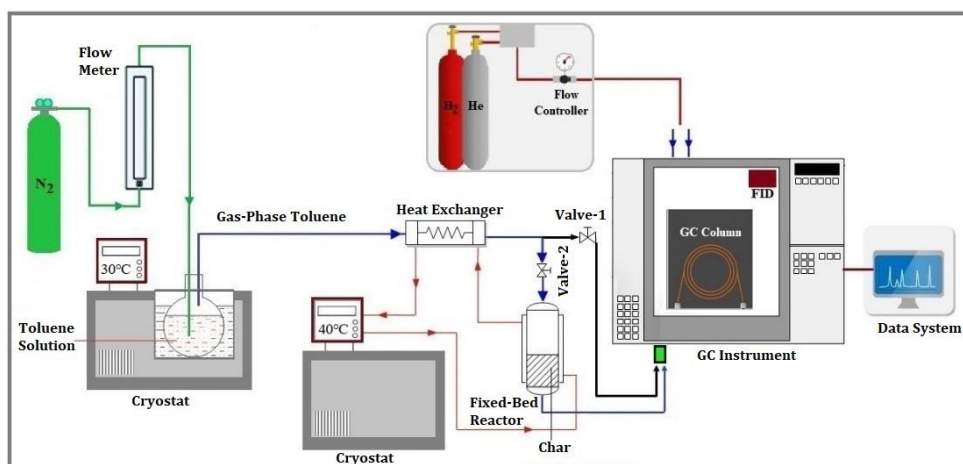

Fig. 1 Schematic diagram of experimental system for the dynamic adsorption of gas-phase toluene onto char

In order to determine the optimum adsorption conditions, the study was carried out under atmospheric pressure at different N_2 flow rates (50-120 mL min^{-1}) as the gas-phase toluene carrier, char amounts (0.25-1.00 g), gas-phase toluene concentrations at the inlet (10.00-15.00 ppm) and temperatures (293-323 K). For this purpose, 300 mL of the toluene solution to be subjected to the vapor dynamic adsorption was placed in a 500 mL glass balloon and then placed in the thermostat set to the study temperature. The gas-phase toluene was introduced into the fixed bed by using N_2 as a carrier gas and it was continuously adsorbed onto the char. The N_2 flow rate during the adsorption process was measured using a volumetric flowmeter. The internal temperature of the jacketed adsorbent, in which the adsorption was carried out, and the gas-phase toluene temperature was kept constant by using the thermostat connected to both the adsorber and the heat exchanger. The concentration of the gas-phase toluene in the N_2 stream at the inlet of the adsorber was analyzed while the valve-2 line was closed and the valve-1 bypass line was open. When the concentration of the gas-phase toluene in the N_2 stream at the inlet of the adsorber reached a steady state, approximately 0.50 g of char was weighed out

and charged into the adsorption column after which the experiments were carried out by turning the valve-1 line to the closed position and the valve-2 line to the open position. The concentrations of the gas-phase toluene in the N_2 stream at the inlet and outlet of the adsorber (10.00, 12.50, 13.50 and 15.00 ppm) were produced using a PID controlled heated thermostat at 293, 303, 313 and 323 ± 0.1 K, respectively. The char particles were supported by microsieve at the outlet of the adsorber. The carrier gas containing a previously arranged concentration of the gas-phase toluene was passed through the column until the gas-phase toluene concentration became stable. The concentrations of the gas-phase toluene at the inlet and outlet of the adsorber were measured by a gas chromatography equipped with a flame ionization detector (GC-FID, GC 910, Buck Scientific) and recorded by a computer. After the dynamic adsorption experiments, the adsorption capacity of the gas-phase toluene onto char was determined by calculating the toluene concentrations in the gas flow before and after it moved through the adsorption column. For this determination, the gas-phase toluene was injected continuously to gas chromatography (GC) and was measured every 10 min. The temperature programming of the GC oven started at T = 80°C after which it was increased at 10°C min^{-1} until it reached 200°C and remained at T = 200°C for 3 min (total of 15 min). The retention time was defined as the closest to the peak of toluene and the determination of gas-phase toluene concentrations was carried out by means of a four-point calibration curve. Analyzes in the experiments were performed at thrice and they showed good reproducibility.

2.4. Measurement of the Adsorption Capacity and the Adsorption Efficiency

The adsorption capacity and adsorption efficiency of the gas-phase toluene onto char obtained from almond shells were measured under different experimental conditions.

The adsorption capacity was determined using the following equation [21]:

$$q_t = \sum_0^n \left[\frac{F}{m} (C_{in} - C_{eff}) \Delta t \right] \qquad (1)$$

Where, q_t (mg g^{-1}) is the adsorption capacity, that is the amount of gas-phase toluene adsorbed onto char, which was integrated from t=0 to t (min), m (g) is the mass of adsorbent, F (L min^{-1}) is the gas flow rate, n is the number of samples taken, C$_{in}$ (ppm) and C$_{eff}$ (ppm) are the concentrations of gas-phase toluene in the N_2 stream at the inlet and outlet (after adsorption) of the adsorber, respectively. In the adsorption process, q_t=qe was achieved when the equilibrium time (t_e) was reached and it refers to the adsorption capacity at equilibrium.

The adsorption efficiency of the gas-phase toluene onto char is defined as follows:

$$\text{Adsorption efficiency (\%)} = \frac{C_{in} - C_e}{C_{in}} \times 100 \qquad (2)$$

Where, C_{in} (ppm) and C_e (ppm) are the concentrations of the gas-phase toluene at the inlet and equilibrium of the adsorber, respectively.

3. Results and Discussion

In this study, the characterization of the char was performed by BET surface area and FTIR measurements. The influences of adsorption conditions on the adsorption process of the gas-phase toluene onto char were determined in a continuous system. In addition, adsorption kinetics, isotherms and thermodynamics of adsorption process were investigated at different temperatures. To demonstrate reproducibility, data in Tables and Figures were marked with error bars.

3.1. Characterization of Char

The structure of the char produced from almond shells was characterized by BET and FTIR. The functional groups of the produced materials were determined with a Bruker Vertex 70 FTIR instrument in the range of 4000–600 cm^{-1} wave number. The FTIR spectra of char adsorbent was analysed in the range of 4000-600 cm^{-1}, and the result was presented in Figure 2. As seen from Figure 2, there are more than one functional group in the structure of char. The peak at 3700 cm^{-1} shows the presence of the OH-functional group bound by hydrogen bonds. The peak at 2380 cm^{-1} indicates the presence of C = C bonds. The peaks in the range of 2250-2000 cm^{-1} are dimmer and show the presence of the COOH functional group. Nitrogen adsorption-desorption of the BET surface area at 77 K was determined by Quantachrome Nova 1200 series instrument. The BET surface area of the char used in this study as adsorbent was determined as 463 m^2 g^{-1}.
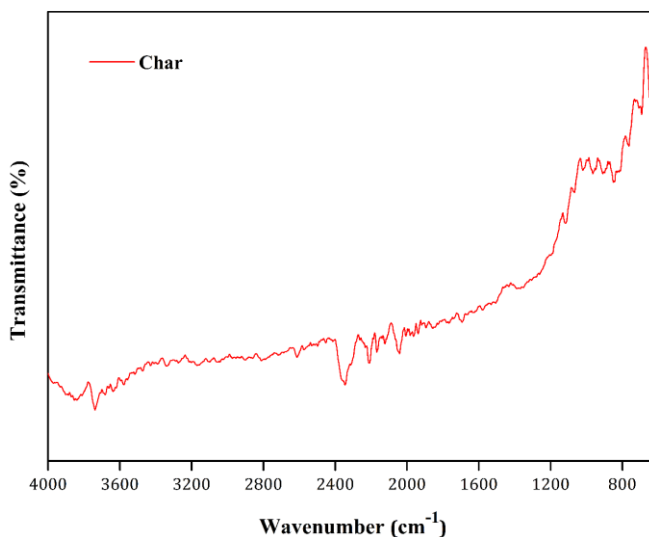

Fig. 2 The FTIR spectra of char adsorbent produced from almond shells

3.2. Influence of Flow Rate on Adsorption Process

In order to illustrate the influence of the flow rate on both the adsorption capacity and the adsorption efficiency of the gas-phase toluene onto char, different flow rates of 50, 75, 100 and 120 mL min^{-1} were used under the experimental conditions of char amount of 0.50 g, temperature of 303 K and concentration of gas-phase toluene at the inlet of 12.50 ppm and the results are given in Figure 3. To determine the equilibrium time of the adsorption, the adsorption capacity was investigated according to the time (0-120 min) (Figure 3a). As shown in Figure 3a, depending on the increase in the flow rate, the adsorption capacity increased. However, in Figure 3b, the adsorption capacity at equilibrium increased with the increasing flow rate, while the adsorption efficiency did not change. This result means that the flow rate in Equation 2, in which the adsorption capacity was determined, changes the adsorption capacity in proportion to the numerical value it has. In other words, it was observed that the amount of toluene adsorbed onto char does not increase at higher flow rates.
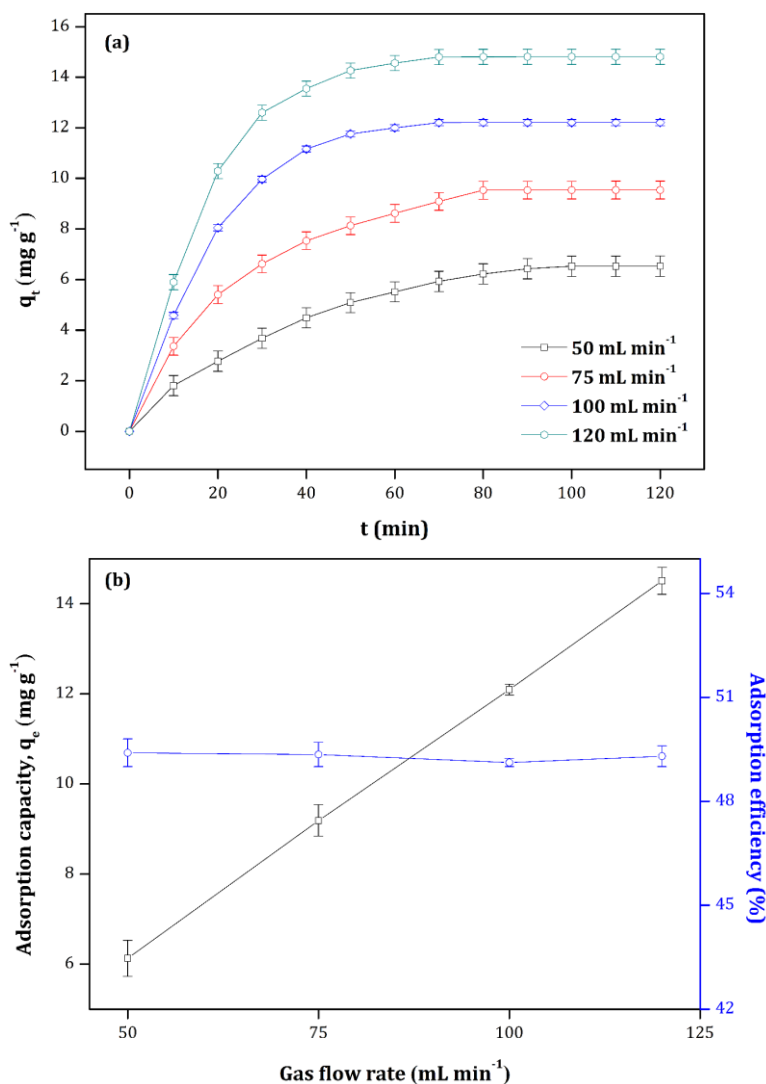
Fig. 3 Influence of flow rate of N$_2$ as the carrier gas on the adsorption capacity with time (a), and the adsorption capacity at equilibrium and the adsorption efficiency (b)

3.3. Influence of the Char Amount on Adsorption

The amount of adsorbent is one of the most important parameters in the adsorption process. In order to illustrate the influence of the char amount on both the adsorption capacity and the adsorption efficiency of the gas-phase toluene onto char, different char amounts of 0.25, 0.50, 0.75 and 1.00 g were used under the experimental conditions of temperature of 303 K, flow rate of 100 mL min^{-1} and concentration of gas-phase toluene at the inlet of 12.50 ppm and the results are given in Figure 4. To determine the adsorption equilibrium time, the adsorption capacity was investigated according to the time (0-120 min) (Figure 4a). Figure 4a shows that an increase in the amount of char caused a decrease in the adsorption capacity. The possible causes of this result can be expressed as the

increase in the amount of char and the increase in the number of activated sites available and the non-saturation of these zones [22], the increase of the activated site ratio of the gas-phase toluene and adsorbent surface and the absence of toluene ions in the medium [23]. As seen in Figure 4b, it was observed that the adsorption capacity at equilibrium decreased with the increasing amount of char, the adsorption efficiency increased up to 0.50 g of char, and did not change with higher amounts of char. An increase in the amount of adsorbent increased the number of active sites available for adsorption, thus increasing the adsorption efficiency [24]. In this study, the minimum amount of adsorbent corresponding to maximum adsorption for char was 0.50 g.
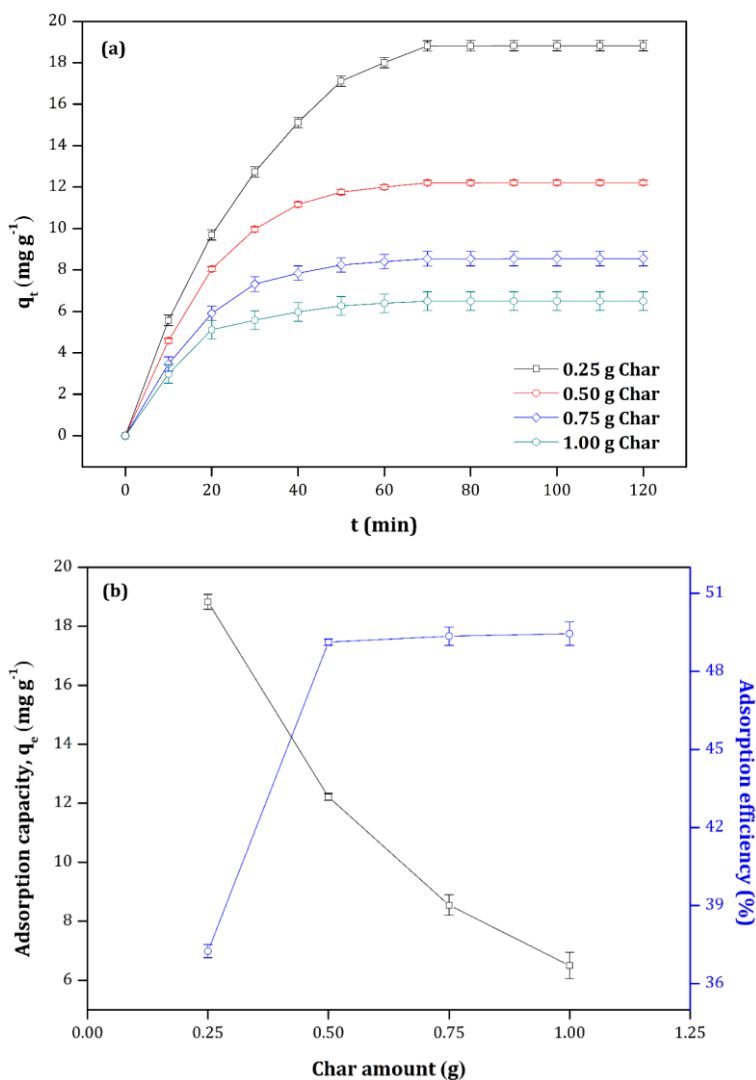

Fig. 4 Influence of the char amount on the adsorption capacity with time (a), and the adsorption capacity at equilibrium and the adsorption efficiency (b)

3.4. Influence of Concentration of Toluene at the inlet on Adsorption Process

In order to illustrate the influence of the concentration of the gas-phase toluene at the inlet on both the adsorption capacity and adsorption efficiency of the gas-phase toluene onto char, different the gas-phase toluene concentrations at the inlet of 10.00, 12.50, 13.50 and 15.00 ppm were used under experimental conditions such as a flow rate of 100 mL min^{-1}, temperature of 303 K and char amount of 0.50 g. The results are given in Figure 5. To determine the adsorption equilibrium time, the adsorption capacity was investigated in accordance with the time (0-120 min) (Figure 5a). As shown in Figure 5a, it was observed that the adsorption capacity increased up to 12.50 ppm and did not change at higher concentrations due to the increase in the gas-phase toluene concentration at the inlet.
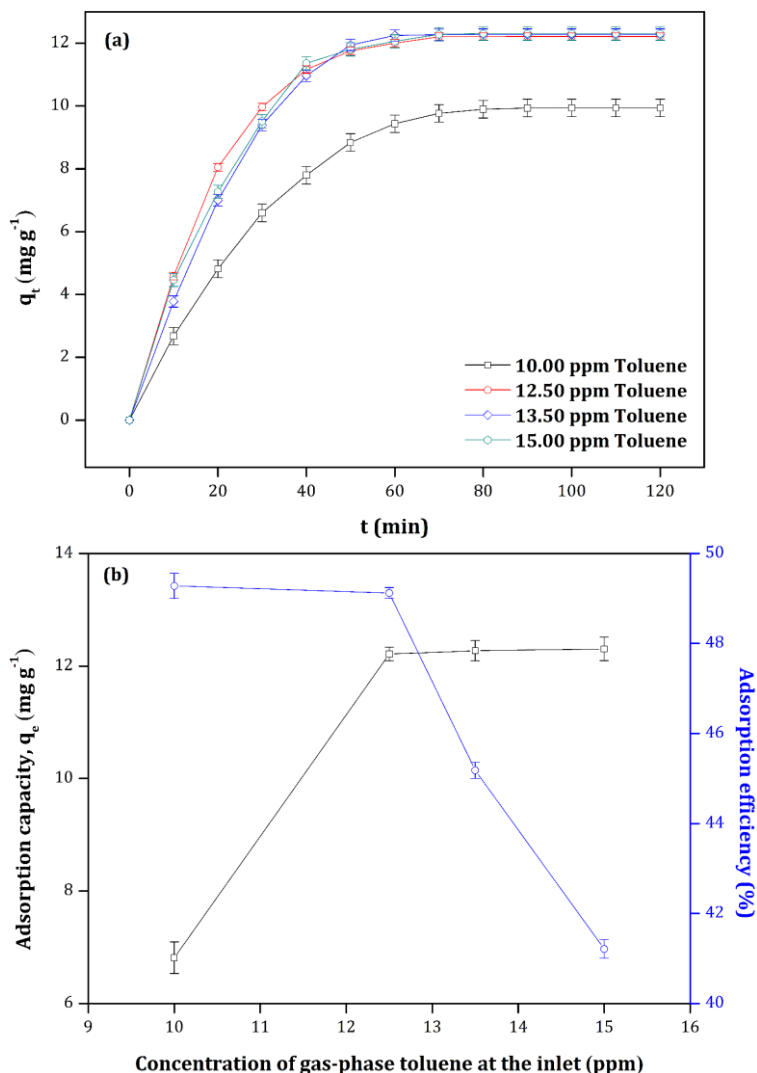

Fig. 5 Influence of concentration on the adsorption capacity with time (a), and the adsorption capacity at equilibrium and the adsorption efficiency (b)

In addition, the increase in the concentration of the gas-phase toluene at the inlet shows that the equilibrium adsorption capacity was reached in a shorter time. These tendencies can be explained with the constant present specific surface area and adsorption area on the char surface and with the fact that an increase in the concentration of the gas-phase toluene at the influent naturally results in a shorter exhaustion time.

In Figure 5b, the increase in the concentration of the gas-phase toluene at the inlet shows that the adsorption capacity at equilibrium increased up to 12.50 ppm and did not change at higher concentrations.

However, the adsorption efficiency was observed to decrease at concentrations greater than 12.451 ppm (Figure 5b). The possible reasons for these circumstances may be the fact that the adsorption capacity, which is a function of the equilibrium concentration, increases with the increasing concentration of the gas-phase toluene at the inlet [25], or with the increase in the number of adsorbate molecules in the vapor that accelerate the adsorption to reach the equilibrium [26].

In all these evaluations, the concentration of the gas-phase toluene at the inlet was taken as 12.50 ppm in other adsorption experiments.

3.5. Influence of Temperature on Adsorption Process

In the adsorption process, temperature plays an important role in the adsorption process. In order to illustrate the influence of the adsorption temperature on both the adsorption capacity and adsorption efficiency of the gas-phase toluene onto char, temperatures of 293, 303, 313 and 323 K were used under experimental conditions such as flow rate of 100 mL min^{-1}, concentration of gas-phase toluene at the inlet of 12.50 ppm and char amount of 0.50 g and the results are given in Figure 6.

To determine the adsorption equilibrium time, the adsorption capacity was investigated according to the time (0-120 min) (Figure 6a). Figure 6a shows that the adsorption capacity did not change until the adsorption temperature reached 303 K and decreased at higher temperatures.

As shown in Figure 6b, both the adsorption capacity at equilibrium and the adsorption efficiency did not change until the adsorption temperature reached 303 K while they decreased at higher temperatures.

Since gas adsorption is an exothermic process, the adsorption capacity decreases with the increasing temperature. This result shows that physical adsorption is a mechanism that separates the gas-phase from liquid phase [27].
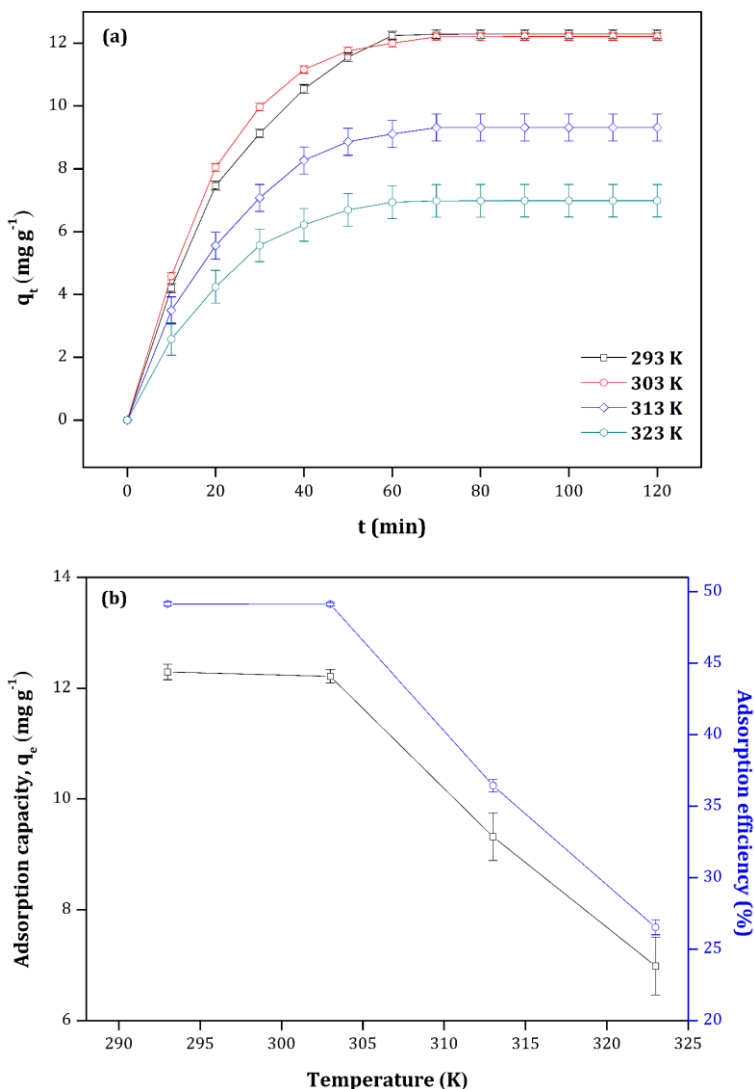
Fig. 6 Influence of temperature on the adsorption capacity with time
(a), and the adsorption capacity at equilibrium and the adsorption
efficiency (b)

3.6. Adsorption Kinetic Studies

Adsorption kinetics is important in understanding the adsorption dynamics between adsorbate and adsorbent. According to adsorption kinetic data, the degree of adsorption, rate constant and the dynamics of adsorption were determined. Important information regarding the design and modeling of the adsorption process can be obtained with kinetic parameters [28]. Pseudo-first-order and pseudo-second-order models were used to determine the adsorption kinetics and mechanisms in this study. The validity of kinetic models was assessed by R^2, regression coefficient, and *Δq (%)* [29]:

$$\Delta q(\%) = 100\sqrt{\frac{\sum[(q_{exp} - q_{mod})/q_{exp}]^2}{N-1}} \tag{3}$$

Where, N is the number of data points, q_{exp} and q_{mod} (mg g^{-1}) are the adsorption capacities of kinetic experiments and models, respectively and Δq is the normalized standard deviation.

The pseudo-first-order kinetic model is the first equation to explain the adsorption capacity and adsorption rate [30]. The pseudo-first-order kinetic model equation [31] is given below:

$$\ln(q_e - q_t) = \ln q_e - k_1 t \tag{4}$$

Where, q_e (mg g^{-1}) and q_t (mg g^{-1}) are the adsorption capacities at equilibrium and at time t, respectively. k_1 (min^{-1}) is the rate constant, and t (min) is the adsorption time. k_1 is calculated from the slope of the plot of $\ln(q_e-q_t)$ against t.

The pseudo-second-order kinetic model equation [32] is given below:

$$\frac{t}{q_t} = \frac{1}{k_2 q_e^2} + \frac{1}{q_e} t \tag{5}$$

Where, k_2 (g mg^{-1} min^{-1}) is the rate constant. q_e and k_2 are calculated from the slope and intercept of the plot of t/q_t against t, respectively.

In order to understand the adsorption process of the gas-phase toluene onto char, pseudo-first-order and pseudo-second-order kinetic models were applied to the experimental data obtained at different temperatures. The linear and non-linear plots of the pseudo-first-order and pseudo-second-order kinetic models are shown in figures 7(a)-(b) and 8(a)-(b), respectively. All kinetic parameters, correlation coefficient (R^2) and Δq (%) values obtained from the linear plots of the kinetic models at different temperatures are listed in Table 1. Figure 7(a)-(b) shows that the pseudo-first-order kinetic model did not give beneficial results for the adsorption of the gas-phase toluene onto char, indicating that it is not in good agreement with the adsorption data. On the other hand, Figure 8(a)-(b) shows that the pseudo-second-order kinetic model gave beneficial results for the adsorption of the gas-phase toluene onto char which shows a satisfactory agreement with the experimental adsorption data. All these results show that the R^2 values of the pseudo-first-order kinetic model showed a weak correlation of the gas-phase toluene adsorption onto char and the Δq values showed a high standard deviation, whereas the R^2 values of the pseudo-second-order kinetic model were higher than 0.98 and the Δq values were less than 3% (Table 1).

Table 1. Kinetic model parameters for the adsorption of gas-phase toluene onto char

| Models	Parameters	Temperature (K)			
		293	303	313	323
Pseudo-first-order	q_e (mg g^{-1})	13.41±0.14	13.25±0.12	9.461±0.43	7.154±0.52
	k_1 (min^{-1})	0.076±0.14	0.074±0.12	0.035±0.43	0.019±0.52
	R^2	0.889±0.14	0.847±0.12	0.874±0.43	0.837±0.52
	Δq (%)	6.187±0.14	8.356±0.12	7.424±0.43	8.773±0.52
Pseudo-second-order	q_e (mg g^{-1})	14.521±0.14	14.35±0.12	10.02±0.43	7.86±0.52
	k_2 (g mg^{-1} min^{-1})	0.0016±0.14	0.005±0.12	0.008±0.43	0.009±0.52
	R^2	0.9999±0.14	0.999±0.12	0.997±0.43	0.998±0.52
	Δq (%)	0.5118±0.14	0.754±0.12	1.356±0.43	1.278±0.52
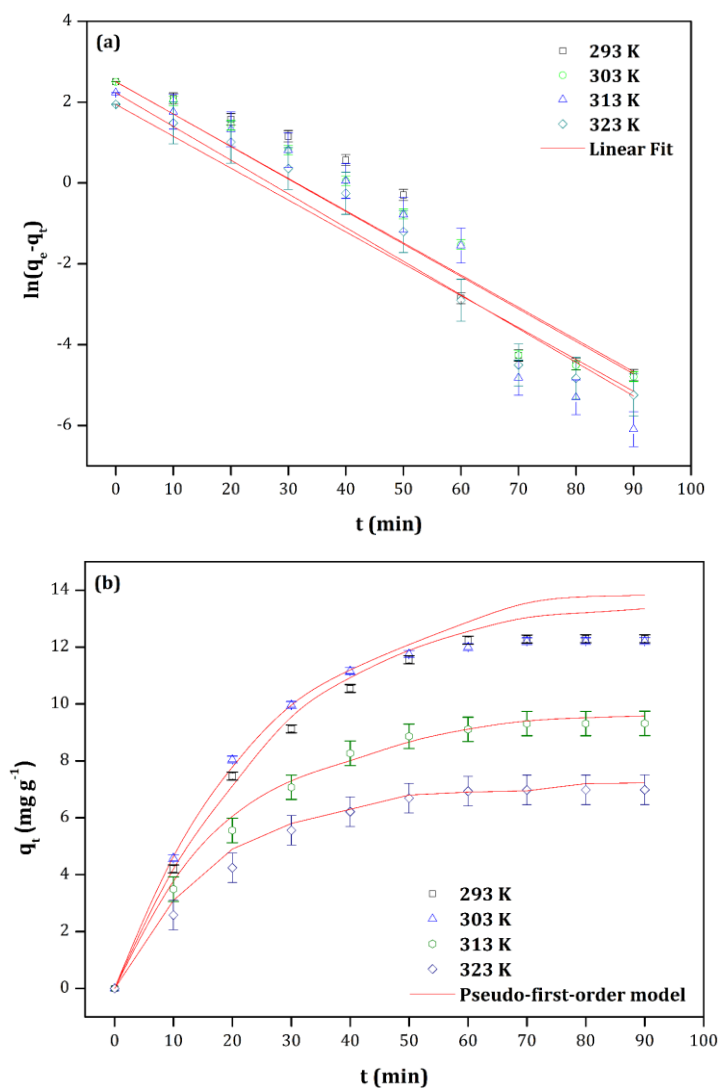
Fig. 7 Pseudo-first-order kinetic model in linear (a) and non-linear (b) methods and experimental kinetics for the adsorption of gas-phase toluene onto char
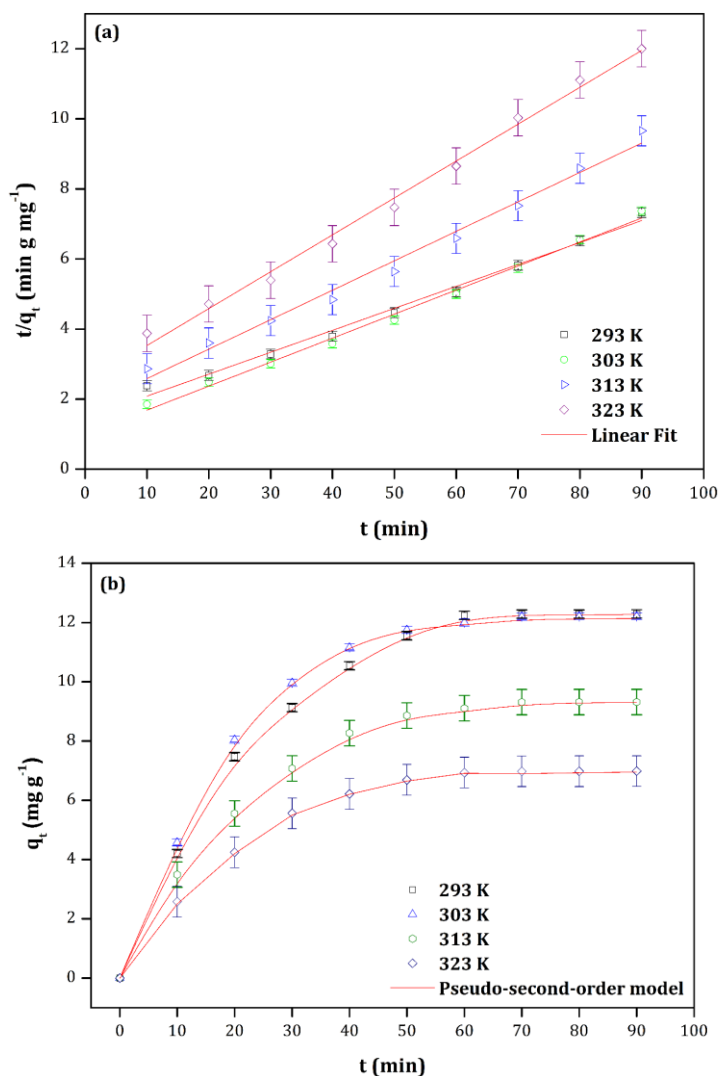
Fig. 8 Pseudo-second-order kinetic model in linear (a) and non-linear (b) methods and experimental kinetics for the adsorption of gas-phase toluene onto char

3.7. Adsorption Isotherm Studies

The most important factors in the interaction between adsorbate and adsorbent are the load and structure of the adsorbent, surface properties of the adsorbent, hydrophobic and hydrophilic structure of the adsorbent, hydrogen bonds, electrostatic interaction, steric effect and Van der Walls forces. The equilibrium studies giving the adsorption capacity of the adsorbent are explained using the adsorption isotherm models [33]. To understand the adsorption process of the gas-phase toluene onto char and to evaluate the equilibrium isotherm, experimental adsorption data obtained at different temperatures were modeled using Langmuir and Freundlich isotherm models. The validity of the isotherm models was assessed by R^2, regression coefficient, and Δq (%).

The Langmuir isotherm model was formed by the adoption of monolayer adsorption. According to this model, monolayer adsorption occurs between the outer surface of the adsorbent and the adsorbate due to the rapid reduction of the distance between the intermolecular forces [34]. The Langmuir isotherm model equation [35] is given below:

$$\frac{C_e}{q_e} = \frac{1}{q_{max}\,K_L} + \frac{C_e}{q_{max}} \tag{6}$$

Where, q_{max} (mg g^{-1}) is the monolayer adsorption capacity, and K_L (L mg^{-1}) is the Langmuir adsorption constant. q_{max} and K_L are calculated from the slope and intercept of the plot of C_e/q_e against C_e, respectively.

The Freundlich isotherm model was developed by adopting adsorption on heterogeneous surfaces. It is accepted that the active areas are reduced with bonding forces [26]. The Freundlich isotherm model equation [36] is given below:

$$\ln q_e = \ln K_F + \frac{1}{n}\ln C_e \tag{7}$$

Where, K_F [(mg/g) (L/mg)$^{1/n}$] is Freundlich adsorption constant. $1/n$ indicates the heterogeneity of data distribution of active centers and is a measure of the adsorption intensity. $1/n$ and K_F are calculated from the slope and intercept of the plot of $\ln q_e$ against $\ln C_e$, respectively.

Plots of Langmuir and Freundlich isotherm models are presented in figures 9 and 10, respectively. All the obtained parameters, correlation coefficient (R^2) and Δq values calculated from the linear plots of the isotherm models are reported in Table 2.

Table 2. Isotherm model parameters for the adsorption of gas-phase toluene onto char

Models	Parameters	Temperature (K)			
		293	303	313	323
Langmuir	q_{max} (mg g^{-1})	15.05±0.14	15.42±0.12	11.12±0.43	9.35±0.52
	K_L (m^3 mg^{-1})	0.058±0.14	0.043±0.12	0.036±0.43	0.029±0.52
	R^2	0.999±0.14	0.998±0.12	0.988±0.43	0.991±0.52
	Δq (%)	1.49±0.14	1.92±0.12	2.98±0.43	2.02±0.52
Fruendlich	K_F [(mg g^{-1}) (m^3 mg^{-1})$^{1/n}$]	3.136±0.14	3.112±0.12	3.005±0.43	2.567±0.52
	$1/n$	0.212±0.14	0.2236±0.12	0.2641±0.43	0.3254±0.52
	R^2	0.749±0.14	0.7436±0.12	0.7358±0.43	0.7284±0.52
	Δq (%)	8.53±0.14	8.56±0.12	10.07±0.43	12.87±0.52

As can be seen from figures 9 and 10, it is clear that the plots of the Langmuir isotherm model fit well with the experimental data, while the plots of Freundlich isotherm model do not fit. Furthermore, as can be seen from Table 2, while the R^2 values for the Freundlich isotherm model for different temperatures, the weak correlation of the gas-phase toluene adsorption onto char and the Δq values show high standard deviation, the R^2 values of the Langmuir isotherm model are 0.98, and Δq values are less than 3%. This result indicates that the surface energy is homogeneously distributed and that single-plate adsorption occurs [37]. The maximum monolayer adsorption capacity (q_{max}) of the char was calculated as 15.42 mg g^{-1} for 303 K. The n parameter obtained from the Freundlich model is always greater than 1, thus, confirming that the adsorption of the gas-phase toluene onto char is a physical adsorption [38]. However, the reduction of both the Freundlich constants, K_F and n (i.e., the increase of $1/n$), by temperature increase confirms that adsorption is feasible at

low temperatures, in other words, low temperatures facilitate the adsorption of the gas-phase toluene onto char [39].
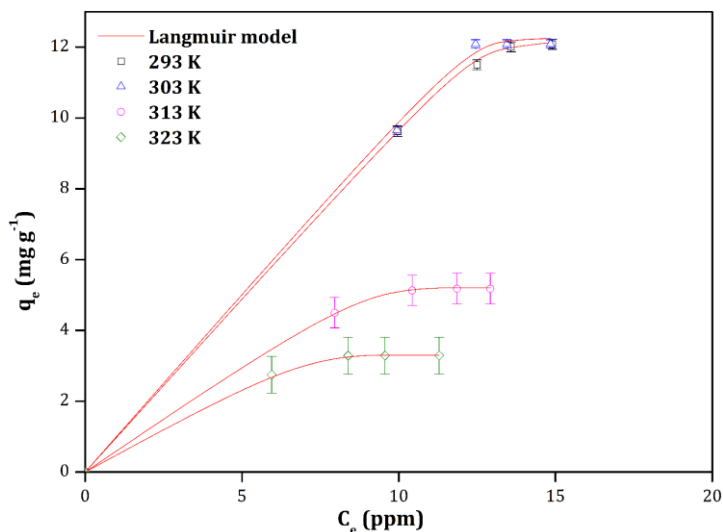

Fig. 9 Adsorption isotherm for the adsorption of gas-phase toluene onto char fitted by Langmuir model at different temperatures
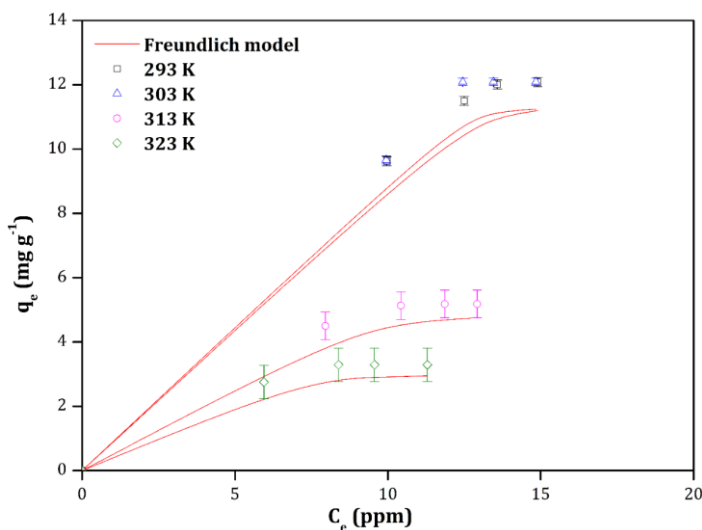

Fig. 10 Adsorption isotherm for the adsorption of gas-phase toluene onto char fitted by Freundlich model at different temperatures

3.8. Adsorption Thermodynamic Studies

The equilibrium state in physical and chemical events in the adsorption process is related to thermodynamics. Whether the adsorption event is an endothermic or exothermic event can be determined in accordance with thermodynamic parameters. Adsorption mechanism can be explained by thermodynamic parameters such as Gibbs free energy

293

change ($\Delta G°$), enthalpy change ($\Delta H°$) and entropy change ($\Delta S°$) [29]. As has been widely reported in the literature [39-41], the thermodynamic laws incorporating experimental data obtained from Langmuir isotherms (the best isotherm model fitted) can be used to determine thermodynamic parameters through the following equations [21]:

$$\Delta G^0 = -RT\ln K_e^{\circ} \qquad (8)$$

$$\Delta G^0 = \Delta H^0 - T\Delta S^0 \qquad (9)$$

Where, R (8.314 J mol^{-1} K^{-1}) is the universal ideal gas constant and T is the absolute temperature in Kelvin (K). K_e° is the thermodynamic equilibrium constant that is dimensionless. The $\Delta G°$ (kJ mol^{-1}) parameter is calculated directly by Equation 8.

The well-known Van't Hoff equation is obtained by incorporating Equation 8 into Equation 9:

$$\ln K_e^{\circ} = \frac{\Delta S^0}{R} - \frac{\Delta H^0}{R}\frac{1}{T} \qquad (10)$$

The $\Delta H°$ (kJ mol^{-1}) and $\Delta S°$ (kJ mol^{-1} K^{-1}) parameters are calculated from the slope and intercept of the plot of $\ln K_e^{\circ}$ against $1/T$, respectively.

In order to determine the thermodynamic parameters, experiments were carried out at four different temperatures: 293, 303, 313 and 323 K. The $\Delta G°$ parameter was calculated directly using Equation 8. The $\Delta H°$ and $\Delta S°$ parameters were determined from the slope and the intercept of the linear plots in Figure 11, respectively. The data of $\ln K_e^{\circ}$ versus $1/T$ were plotted and are shown in Figure 11. The calculated Gibbs Free Energy ($\Delta G°$), enthalpy change ($\Delta H°$) and entropy change ($\Delta S°$) values are presented in Table 3. In Table 3, the negative sign of $\Delta G°$ indicates that the adsorption process was appropriate and spontaneous [42]. The $\Delta G°$ values between -20 kJ mol^{-1} and 0 kJ mol^{-1} were reduced to the physical adsorption range [43]. This result shows that physical adsorption was the dominant mechanism for the adsorption of the gas-phase toluene onto char. The $\Delta H°$ value for the adsorption process was calculated as -17.18 kJ mol^{-1}. The negative value of the calculated $\Delta H°$ indicates that the adsorption process was exothermic. Furthermore, the magnitude of $\Delta H°$ (<20 kJ mol^{-1}) indicates that physical adsorption was predominant [39]. The negative value of $\Delta S°$ indicates that the entropy of the system decreased. This means that the disorder of the system during the adsorption process and the randomization of the adsorbate at the solid/gas interface were reduced [30]. his is because, the gas-phase toluene molecules pass from a random step to a regular step (on the surface of the adsorbent).

Table 3. Thermodynamics parameters for the adsorption of gas-phase toluene onto char

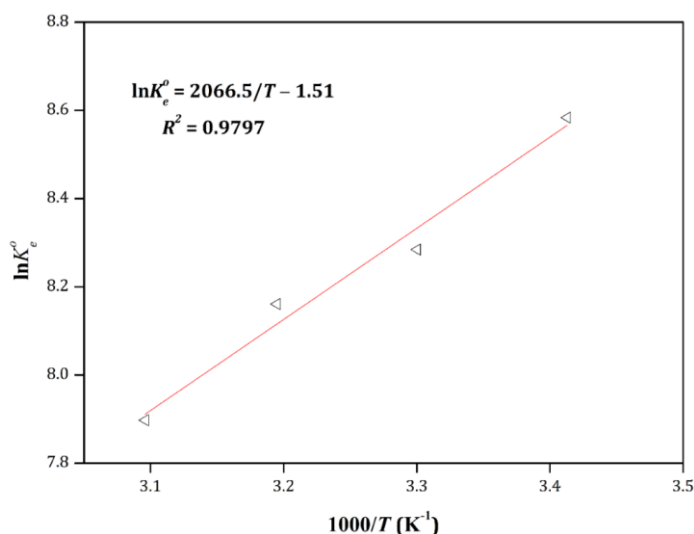| T (K)	$\Delta G°$ (kJ mol^{-1})	$\Delta H°$ (kJ mol^{-1})	$\Delta S°$ (kJ mol^{-1} K^{-1})
293	-6.936±0.14	-17.181	-0.025
303	-7.927±0.12		
313	-8.651±0.43		
323	-9.489±0.52		

Fig. 11 Plots of $\ln K_e^\circ$ versus $1/T$ for the estimation of thermodynamic parameters

4. Conclusions

Toluene is a VOC which is abundantly found in the environment. Toluene is the primary material used in chemical process industries and is often used as a raw material in the production of many chemicals and as a solvent in many engineering processes. The material of char, which is used as an adsorbent, is produced from almond shells. Almond shells, which are abundant and low-cost residues, are suitable to be used as a raw material for the preparation of char. In this study, the adsorption of gas-phase toluene onto char was studied in a dynamic system by using a laboratory-scale fixed-bed reactor under atmospheric pressure. Adsorption parameters such as N_2 flow rate as the gas-phase toluene carrier, char amount, gas-phase toluene concentration at the inlet, and adsorption temperature play an important role in both the adsorption capacity and adsorption efficiency of the gas-phase toluene onto char.

Experimental results showed that the adsorption capacity decreased with increasing temperatures and the amount of char while it increased with the gas flow rate and the concentration of the gas-phase toluene at the inlet. In addition, results of gas flow rate of 100 mL min^{-1}, char amount of 0.50 g, concentration of gas-phase toluene at the inlet of 12.50 ppm, and temperature of 303 K showed good reproducibility. Adsorption kinetics data were analyzed using pseudo-first-order and pseudo-second-order models. The adsorption of the gas-phase toluene onto char can be well represented by the pseudo-second-order kinetic model. Equilibrium isotherm data were analyzed by the Langmuir and Freundlich isotherm models and the results indicated that the adsorption process was described well by the Langmuir isotherm model. The maximum monolayer adsorption capacity (q_{max}) of the char was determined as 15.42 mg g^{-1} for 303 K. Thermodynamic parameters such as ΔG° = -7.93 kJ mol^{-1}, ΔH° = -17.18 kJ mol^{-1}, ΔS° = -0.013 kJ mol^{-1} K^{-1} showed that the adsorption process of the gas-phase toluene onto char was spontaneous, exothermic and physical. The results showed that the material of the char produced from almond shells could be used as a biosorbent to remove the material of the gas-phase toluene from various industrial and natural sources through the adsorption method.

References

[1] Koppmann R. Volatile Organic Compounds in the Atmopshere. UK.: Blackwell Publishing Ltd.; 2007. https://doi.org/10.1002/9780470988657

[2] Ghoshal AK, Manjare SD. Selection of appropriate adsorption technique for recovery of VOCs: an analysis. Journal of Loss Prevention in the Process Industries. 2002;15(6):413-421. https://doi.org/10.1016/S0950-4230(02)00042-6

[3] Khan FI, Kr. Ghoshal A. Removal of Volatile Organic Compounds from polluted air. Journal of Loss Prevention in the Process Industries. 2000;13(6):527-545. https://doi.org/10.1016/S0950-4230(00)00007-3

[4] Pires J, Carvalho A, de Carvalho MB. Adsorption of volatile organic compounds in Y zeolites and pillared clays. Microporous and Mesoporous Materials. 2001;43(3):277-287. https://doi.org/10.1016/S1387-1811(01)00207-4

[5] Srivastava NC, Eames IW. A review of adsorbents and adsorbates in solid–vapour adsorption heat pump systems. Applied Thermal Engineering. 1998;18(9):707-714. https://doi.org/10.1016/S1359-4311(97)00106-3

[6] Tsai W-T. A review of environmental hazards and adsorption recovery of cleaning solvent hydrochlorofluorocarbons (HCFCs). Journal of Loss Prevention in the Process Industries. 2002;15(2):147-157. https://doi.org/10.1016/S0950-4230(01)00023-7

[7] Hindarso H, Ismadji S, Wicaksana F, Mudjijati, Indraswati N. Adsorption of Benzene and Toluene from Aqueous Solution onto Granular Activated Carbon. Journal of Chemical & Engineering Data. 2001;46(4):788-791. https://doi.org/10.1021/je000176g

[8] Jones AP. Indoor air quality and health. Atmospheric Environment. 1999;33(28):4535-4564. https://doi.org/10.1016/S1352-2310(99)00272-1

[9] Gupta VK, Verma N. Removal of volatile organic compounds by cryogenic condensation followed by adsorption. Chemical Engineering Science. 2002;57(14):2679-2696. https://doi.org/10.1016/S0009-2509(02)00158-6

[10] Hwang KS, Dae Ki C, Sung Yong G, Sung Yong C. Adsorption and thermal regeneration of methylene chloride vapor on an activated carbon bed. Chemical Engineering Science. 1997;52(7):1111-1123. https://doi.org/10.1016/S0009-2509(96)00470-8

[11] Naidu G, Jeong S, Johir MAH, Fane AG, Kandasamy J, Vigneswaran S. Rubidium extraction from seawater brine by an integrated membrane distillation-selective sorption system. Water Research. 2017;123:321-331. https://doi.org/10.1016/j.watres.2017.06.078

[12] Shahmirzadi MAA, Hosseini SS, Tan NR. Enhancing removal and recovery of magnesium from aqueous solutions by using modified zeolite and bentonite and process optimization. Korean Journal of Chemical Engineering. 2016;33(12):3529-3540. https://doi.org/10.1007/s11814-016-0218-z

[13] Lillo-Ródenas MA, Cazorla-Amorós D, Linares-Solano A. Behaviour of activated carbons with different pore size distributions and surface oxygen groups for benzene and toluene adsorption at low concentrations. Carbon. 2005;43(8):1758-1767. https://doi.org/10.1016/j.carbon.2005.02.023

[14] Roop Chand Bansal, Goyal M. Activated Carbon Adsorption. 1 st ed. Boca Raton: Taylor & Francis Group; 2005. 263-265 p.

[15] Parra MA, Elustondo D, Bermejo R, Santamaría JM. Quantification of indoor and outdoor volatile organic compounds (VOCs) in pubs and cafés in Pamplona, Spain. Atmospheric Environment. 2008;42(27):6647-6654. https://doi.org/10.1016/j.atmosenv.2008.04.026

[16] Ruthven DM. Principles of Adsorption and Adsorption Processes. New York: John Wiley; 1984.

[17] Allen RWK, D Archer E, MacInnes J. Adsorption by Particles Injected into a Gas Stream. Chemical Engineering Journal - CHEM ENG J. 2001;83:165-174. https://doi.org/10.1016/S1385-8947(00)00264-3

[18] Allen RWK, Archer ED, MacInnes JM. Theoretical account of a dry sorption injection experiment. AIChE. 2001;47(12):2684-2695. https://doi.org/10.1002/aic.690471208

[19] Archer ED, Allen RWK, MacInnes JM. Measurements of VOC take-up by adsorbing particles in a gas stream. Filtration & Separation. 2000;37(10):32-39. https://doi.org/10.1016/S0015-1882(00)80250-5

[20] Balathanigaimani MS, Shim W-G, Lee M-J, Lee J-W, Moon H. Adsorption Isotherms of Benzene and Toluene on Corn Grain-Based Carbon Monolith at (303.15, 313.15, and 323.15) K. Journal of Chemical & Engineering Data. 2008;53(3):732-736. https://doi.org/10.1021/je700575g

[21] Kutluay S, Baytar O, Şahin Ö. Equilibrium, kinetic and thermodynamic studies for dynamic adsorption of benzene in gas phase onto activated carbon produced from elaeagnus angustifolia seeds. Journal of Environmental Chemical Engineering. 2019;7(2):102947. https://doi.org/10.1016/j.jece.2019.102947

[22] Hassan AF, Abdel-Mohsen AM, Fouda MMG. Comparative study of calcium alginate, activated carbon, and their composite beads on methylene blue adsorption. Carbohydrate Polymers. 2014; 102:192-198. https://doi.org/10.1016/j.carbpol.2013.10.104

[23] Noorimotlagh Z, Darvishi Cheshmeh Soltani R, Khataee AR, Shahriyar S, Nourmoradi H. Adsorption of a textile dye in aqueous phase using mesoporous activated carbon prepared from Iranian milk vetch. Journal of the Taiwan Institute of Chemical Engineers. 2014;45(4):1783-1791. https://doi.org/10.1016/j.jtice.2014.02.017

[24] Bazrafshan E., Faridi H., M.F. K, A.H. M. Arsenic removal from aqueous environments using moringa peregrina seed extract as a natural coagulant. Asian Journal of Chemistry. 2013;25:3557-3561. https://doi.org/10.14233/ajchem.2013.13647

[25] de Luna MDG, Flores ED, Genuino DAD, Futalan CM, Wan M-W. Adsorption of Eriochrome Black T (EBT) dye using activated carbon prepared from waste rice hulls—Optimization, isotherm and kinetic studies. Journal of the Taiwan Institute of Chemical Engineers. 2013;44(4):646-653. https://doi.org/10.1016/j.jtice.2013.01.010

[26] Hameed BH, El-Khaiary MI. Equilibrium, kinetics and mechanism of malachite green adsorption on activated carbon prepared from bamboo by K2CO3 activation and subsequent gasification with CO2. Journal of Hazardous Materials. 2008;157(2):344-351. https://doi.org/10.1016/j.jhazmat.2007.12.105

[27] Ramirez D, Qi S, Rood MJ, Hay KJ. Equilibrium and Heat of Adsorption for Organic Vapors and Activated Carbons. Environmental Science & Technology. 2005;39(15):5864-5871. https://doi.org/10.1021/es048144r

[28] M. M. Vargas A, L. Cazetta A, Kunita M, L. Silva T, Almeida V. Adsorption of methylene blue on activated carbon produced from flamboyant pods (Delonix regia): Study of adsorption isotherms and kinetic models. Chemical Engineering Journal. 2011;168(2):722-730. https://doi.org/10.1016/j.cej.2011.01.067

[29] Ammendola P, Raganati F, Chirone R. CO2 adsorption on a fine activated carbon in a sound assisted fluidized bed: Thermodynamics and kinetics. Chemical Engineering Journal. 2017;322:302-313. https://doi.org/10.1016/j.cej.2017.04.037

[30] Gürses A, Doğar Ç, Yalçın M, Açıkyıldız M, Bayrak R, Karaca S. The adsorption kinetics of the cationic dye, methylene blue, onto clay. Journal of Hazardous Materials. 2006;131(1):217-228. https://doi.org/10.1016/j.jhazmat.2005.09.03

[31] Sari A, Tuzen M, Citak D, Soylak M. Equilibrium, kinetic and thermodynamic studies of adsorption of Pb(II) from aqueous solution onto Turkish kaolinite clay. Journal of Hazardous Materials. 2007; 149(2):283-291. https://doi.org/10.1016/j.jhazmat.2007.03.078

[32] Dursun AY, Kalayci ÇS. Equilibrium, kinetic and thermodynamic studies on the adsorption of phenol onto chitin. Journal of Hazardous Materials. 2005;123(1):151-157. https://doi.org/10.1016/j.jhazmat.2005.03.034

[33] Magdy YH, Daifullah AAM. Adsorption of a basic dye from aqueous solutions onto sugar-industry-mud in two modes of operations. Waste Management. 1998;18(4):219-226. https://doi.org/10.1016/S0956-053X(98)00022-1

[34] El-Bindary AA, Hussien MA, Diab MA, Eessa AM. Adsorption of Acid Yellow 99 by polyacrylonitrile/activated carbon composite: Kinetics, thermodynamics and isotherm studies. Journal of Molecular Liquids. 2014;197:236-242. https://doi.org/10.1016/j.molliq.2014.05.003

[35] Langmuir I. The adsorption of gases on plane surfaces of glass, mica and platinum. J Am Chem Soc 1918;40:1361–1368. https://doi.org/10.1021/ja02242a004

[36] Freundlich HMF. Over the Adsorption in Solution. The Journal of Physical Chemistry. 1906;57:385-471.

[37] Guo Y, Li Y, Zhu T, Wang J, Ye M. Modeling of dioxin adsorption on activated carbon. Chemical Engineering Journal. 2016;283:1210-1215. https://doi.org/10.1016/j.cej.2015.08.067

[38] A.O D, Olalekan A, Olatunya A, Dada AO. Langmuir, Freundlich, Temkin and Dubinin–Radushkevich Isotherms Studies of Equilibrium Sorption of Zn 2+ Unto Phosphoric Acid Modified Rice Husk. IOSR Journal of Applied Chemistry (IOSR-JAC). 2012;3:38-45. https://doi.org/10.9790/5736-0313845

[39] A.A. Adelodun, J.C. Ngila, D.-G. Kim, Jo YM. Isotherm, Thermodynamic and Kinetic Studies of Selective CO2 Adsorption on Chemically Modified Carbon Surfaces. Aerosol and Air Quality Research. 2016:3312–3329.

[40] Hauchhum L, Mahanta P. Carbon dioxide adsorption on zeolites and activated carbon by pressure swing adsorption in a fixed bed. International Journal of Energy and Environmental Engineering. 2014;5(4):349-356. https://doi.org/10.1007/s40095-014-0131-3

[41] Singh VK, Anil Kumar E. Measurement and analysis of adsorption isotherms of CO2 on activated carbon. Applied Thermal Engineering. 2016;97:77-86. https://doi.org/10.1016/j.applthermaleng.2015.10.052

[42] He J, Hong S, Zhang L, Gan F, Ho Y-S. Equilibrium and Thermodynamic Parameters of Adsorption of Methylene Blue onto Rectorite. Fresenius Environmental Bulletin. 2010;19:2651–2656.

[43] Duranoğlu D, Trochimczuk AW, Beker U. Kinetics and thermodynamics of hexavalent chromium adsorption onto activated carbon derived from acrylonitrile-divinylbenzene copolymer. Chemical Engineering Journal. 2012;187:193-202. https://doi.org/10.1016/j.cej.2012.01.120